Polarization VLBI observations at 1.6 GHz and 5 GHz with the HALCA satellite: first results from in-orbit checkout observations

Polarization Study Team (PST)

C. Flatters[1]
D. Gabuzda[2]
H. Hirabayashi[3]
S. Horiuchi[4]
M. Inoue[4]
A. Kemball[1] (Chair)
H. Kobayashi[3]
G. Moellenbrock[3]
Y. Murata[3]

1: National Radio Astronomy Observatory (NRAO), Socorro, NM
2: Astro Space Center, Lebedev Physical Institute, Moscow
3: Institute of Space and Astronautical Science, Tokyo
4: Nobeyama Radio Observatory, Mitaka

April 6, 1998

Abstract

We present and discuss the results of 1.6 GHz and 5 GHz test polarization observations obtained with HALCA, the VLBA and phased VLA, specifically to evaluate the feasibility of calibrating and imaging HALCA polarization data. Our analysis indicates that centimeter-wavelength polarization imaging using HALCA is technically viable for sources with sufficiently high correlated polarized flux densities. The test data are limited, but provide evidence that the HALCA instrumental polarization is constant on time-scales of $\sim 5-6$ hours.

Contents

1 Introduction

Polarization VLBI observations with the HALCA satellite offer unique possibilities for investigating the polarization properties of compact extra-galactic radio sources, if such observations can be made technically feasible. The increased spatial resolution this offers at centimeter wavelengths over that possible with ground arrays at comparable frequencies, allows an investigation of the fine-scale polarization structure of such objects at unprecedented resolution. This is particularly useful near the core, in examining the magnetic field and shock structure of the inner jet, in addition to the kinematics and jet geometry in this region. An important contribution offered by higher resolution polarization observations at centimeter wavelengths is the possibility of exploring the known relationship between polarization morphology and optical class (Gabuzda *et al.* 1992) closer to the core. Also, higher resolution polarization observations at 1.6 GHz and 5 GHz can be more readily compared to ground array observations at higher frequencies, in order to study the distribution of Faraday rotation in compact extra-galactic radio sources.

The Polarization Study Team (PST) was formed to investigate the feasibility of polarization VLBI observations with the HALCA satellite, and to recommend scheduling and data reduction strategies for such observations. Several test observations were conducted during the in-orbit checkout period to explore these questions, and we summarize the analysis of the first directed PST test observations (projects VT824 and VT825) in this note. The HALCA satellite is sensitive only to left-circular polarization (LCP), but ground-array recording in dual-circular polarization permits information to be obtained on cross-polarized correlations on the space baselines, and consequently the linear polarization of the source under study.

Candidate PST test observations were confined to those in-orbit checkout projects which were to be recorded in VLBA mode, scheduled for correlation at the National Radio Astronomy Observatory (NRAO) in Socorro, and in which the phased VLA or Effelsberg 100m telescope was to participate. Further selection criteria were applied based on logistical constraints and the suitability of the target source as a polarization calibrator. In-orbit checkout projects that were selected in this way were observed as scheduled but with the sole modification that dual-circular polarization was recorded on the ground array. The primary objective of the projects was thus not affected. Logistically, this doubled the ground array record rate to 256 Mbps. A second correlator pass was scheduled to extract the full cross-polarized information. In addition to the projects selected on this basis, directed polarization test observations were scheduled during the in-orbit checkout period, in which the target source was chosen by the PST based solely on its suitability as a polarization calibrator. The two categories of PST test observations will be referred to as secondary and primary test observations, respectively. Source selection for the primary PST test observations was subject to the scheduling constraints applicable to the spacecraft orbit at the time of observation.

This note in the main concerns the first successful primary PST test observations (VT824 and VT825). The target source in this case was 4C39.25, and the observations were conducted on successive days at 1.6 GHz and 5 GHz, with the first observation on 22 October 1997.

This note outlines the technical considerations applicable to polarization observations with HALCA (section 2), and describes the details of the PST test observations in section 3. The data reduction method is described in section 4 along with the results, and the discussion and conclusions are given in section 5.

2 Orbiting polarization VLBI

Orbiting polarization VLBI observations with the HALCA satellite are distinct from conventional ground-based polarization observations primarily in terms of sensitivity and spatial resolution. In addition, the HALCA antenna is sensitive only to left-circularly polarized incident radiation, resulting in asymmetric polarization sampling for the array as a whole, which is of particular relevance where the cross-polarized correlations are concerned. A further consideration is that for important operational reasons the satellite cannot easily be switched between pointings on short time scales, and thus conventional polarization calibration using secondary sources is not possible. Note also that the HALCA parallactic angle is constant within a given pointing. A discussion of the HALCA parallactic angle is given by Kogan (1997).

Sensitivity is important for polarization VLBI, as compact extra-galactic radio sources are typically only linearly polarized at the level of several percent of the Stokes I flux density. The nominal system equivalent flux density (SEFD) for the HALCA satellite is 15300 Jy at 5 GHz and 17400 Jy at 1.6 GHz (AO2 Proposers Guide, 1998). The rms sensitivity between HALCA and a single 25m VLBA antenna, for which a SEFD of 300 Jy is adopted, is thus approximately 7 times lower than for a single baseline between two VLBA antennas. In addition, the spatial resolution, which is typically 3 times higher than for ground arrays at comparable frequencies, implies lower correlated flux densities in general, which is a further important consideration in assessing the detectability of linearly polarized emission. The higher spatial resolution also impacts the complexity of polarization calibration, in which an estimate of the polarization structure of the source used for calibration purposes is required. Several techniques exist to address this problem, and this question is discussed in further detail below in the consideration of feed calibration strategies.

The asymmetric polarization sampling is not in and of itself a technical obstacle, and has been encountered in ground arrays before. It does require however that the Stokes Q and U data be imaged and deconvolved in a full complex form, as the conventional Hermitian relation is not valid in this case. Software already exists to deal with this, and has been used in processing previous network polarization observations. The constant parallactic angle does not present special difficulties either (compare equatorially mounted ground antennas), but has an impact on feed calibration strategies discussed below.

Feed calibration techniques for polarization VLBI have been the subject of extensive study (Cotton *et al.* 1984, Roberts *et al.* 1984, Roberts *et al.* 1994, Kemball *et al.* 1995, Leppanen 1995) and they are not reviewed in detail here. All techniques of this nature have several key elements in common. The cross-polarized correlations (RL and LR) contain joint information on the source linear polarization and the instrumental polarization (D-term leakage factor) at each antenna in each polarization. Parallactic angle variation allows the separation of these two contributions under certain circumstances.

Assuming zero circular and weak linear polarization, the measured and gain-calibrated cross-hand visibilities on baseline 1-2 (where antenna 1 is an alt-az mounted ground telescope and antenna 2 is HALCA) can be written in a linear approximation as:

$$R_1 L_2^* = \tilde{P}_{12} + D_{1R}\tilde{I}_{12}e^{2i\phi_1} + D_{2L}^*\tilde{I}_{12}e^{2i\phi_2}.$$

$\tilde{P}_{12}$ and $\tilde{I}_{12}$ are the true polarized and total flux density (correlated) on the baseline in question, D_{1R} is the D-term for antenna 1 (leakage of L into R), D_{2L} is the D-term for antenna 2 (leakage of R into L), and ϕ_2 is the parallactic angle of antenna 2 (which for HALCA remains constant during a single observation, unlike alt-az mounted ground telescopes).

The higher resolution applicable to VLBI observations makes it less likely that a point source model can be used for the source polarization, as may often be the assumption for connected-element arrays. In this case a model approximation needs to be adopted for the unknown source polarization, unless the source is known to have negligible linear polarization at the observing frequency. The various techniques model the source linear polarization in different ways. This includes taking the linear polarization to be a scaled form of the Stokes I emission, either for individual components or for the image as a whole. Some techniques are iterative, while others use the ratio of cross-polarized to parallel-hand data in parameter estimation.

Feed calibration for HALCA observations may reasonably be approached through several methods. Although the spacecraft parallactic angle is constant per pointing, there is still parallactic angle variation on baselines to alt-azimuth ground antennas and the same basic techniques can be used. The higher spatial resolution makes the modeling of the source linear polarization more difficult, particularly as only the space baselines may be providing information on the fine-scale polarization structure of the source. The first-order approach to feed calibration would be to solve for the ground-based and HALCA D-terms simultaneously, as is done in conventional polarization VLBI. More sophisticated approaches would include an incremental solution for the D-terms, solving first on the ground where the polarization leakage is well-constrained, and then for HALCA, keeping the ground-based D-terms fixed. A further approach would be to apply a uv-range cutoff in the input data to use only space baselines of nearly comparable resolution to the ground array in the feed D-term solution. This minimizes the coupling between the unknown HALCA D-term and the unknown fine-scale polarization structure of the source. We consider the applicability of some of these approaches in this note, as applied to existing in-orbit checkout observations.

3 PST observations

The policy regarding PST observations is discussed in section 1 above. The observations conducted to date are listed in Table 1, which shows the nominal schedule without reference to tracking station failures. Actual tracking times obtained for each project are given in Table 2.

Source selection for the secondary test observations (VT136, VT801, VT812) was not under the control of the PST. Subject to scheduling constraints, there was control over the target sources for the primary test observations however. The source 1334-127 was chosen for project V025C as it is known to be compact at 5 GHz, is a BL_Lac object and has linear polarization of $\sim 3.5 - 4.5\%$. Unfortunately all tracking passes were lost in this project. For the replacement observations (VT824, VT825) the best candidate polarization calibrator available at that time was 4C39.25. This quasar was chosen primarily for its high flux density ($\sim$ 11 Jy at 5 GHz), low linear polarization ($< 1\%$) and relatively compact structure. Results of ground-based VLBI observations have been reported by Marcaide *et al.* 1994, Alberdi *et al.* 1993 and Alberdi *et al.* 1998. The source is known to have E-W structure but most polarization appears to originate near the core or inner jet region.

Project	Type[1]	Date	Start (UT)	End (UT)	Frequency (MHz)	BW/polzn (MHz)	Source	Ground array
VT136	S	22 May 97	03h15	11h27	1640-1672	32	1519-273	Y27, VLBA
VT801	S	04 Jun 97	18h31	05h40	1634-1666	32	1156+295	Eb, EVN[2], VLBA
V025C	P	13 Jul 97	21h00	06h00	4962-4994	32	1334-127	Y27, VLBA
VT812	S	18 Jul 97	03h00	10h58	1648-1664	16	1921-293	Y27, VLBA
					4978-4994	16		
VT824	P	22 Oct 97	07h38	21h30	1648-1664	16/32[3]	4C39.25	Y27, VLBA
VT825	P	23 Oct 97	07h00	22h00	4962-4994	32	4C39.25	Y27, VLBA

Table 1: Scheduled PST test observations. *Notes: [1]: S=secondary,P=primary; [2]: Jb,Mc,Nt,On,Tr,Wb; [3]: partial 16 MHz due to observing error.*

Project	Tracking stn.	Start (UT)	End (UT)	Total (h)
VT136	Greenbank	03h15	06h15	3.0
VT801	Greenbank	03h05	05h30	2.4
V025C	*no tracking*	-	-	0
VT812	Goldstone	09h40	11h00	
	Greenbank	03h00	04h45	3.1
VT824	Tidbinbilla	07h40	09h00	
	Madrid	12h15	14h08	
	Greenbank	18h35	20h30	5.1
VT825	Madrid	07h14	08h04	
	Madrid	13h42	15h35	2.7

Table 2: PST test observation tracking pass coverage

The scheduling strategy for projects VT824 and VT825 involved observing the target source 4C39.25 continuously during the HALCA tracking passes, and less frequently during the ground-array only segments. This allowed more targeted utilization of the allocated tapes. Secondary ground-array polarization calibrators were added to the schedule during these segments to allow redundant ground-array polarization calibration. These sources were DA193 and 0J287 in project VT825 and OJ287 alone in project VT824. The source 3C286 was added for absolute polarization calibration of the phased VLA, and as a reference for the VLA flux density scale. The VLA was auto-phased on the target 4C39.25 in project VT825, but a reference source 0839+187 was used in project VT824 to phase up the VLA. This doubled as a secondary VLA polarization calibrator. There was no net subarraying in either project.

The VLBA recording mode adopted for the PST observations involved the recording of two 16 MHz upper-sideband baseband channels per circular polarization, in two-bit sampling and with a contiguous frequency range in each polarization. The total record rate was 256 Mbps, with a duration of 5h08m per thin tape. This is a two-bit mode with 1:4 fan-out, and current correlator software permits polarization correlation in this mode. The polarization sequence in the baseband converters was (L,L,R,R), which can be correlated in full polarization if the barrel-roll is turned off. The tracking stations record only the two LCP baseband channels in a 128 Mbps mode. Current VLBA correlator software permits full polarization correlation between the tracking stations recording only one polarization and other ground stations recording both RCP and LCP. Only two of the four resulting correlations for baselines involving HALCA contain the desired data (LL and either RL or LR, depending on whether HALCA is the first or second antenna); the other two correlations (RR and the remaining cross-hand correlation) are mis-labeled, and contain redundant data. In the first PST test observations it was checked that the redundant data obey the expected equivalence relations. It is noted also that the polarization sequence in the baseband assignments need not be (L,L,R,R) but can in fact be arbitrary if the barrel-roll is disabled. For modes with the barrel-roll enabled the polarization pairs (R,L) should be adjacent.

All PST test observations were correlated separately in full polarization. For secondary test observations this was done in a later pass after the initial LL correlation. All PST observations discussed here have also been re-correlated after an early VLBA correlator bug in (u,v,w) computation and time control file (TCF) interpolation was identified and corrected.

4 Data reduction and results

Early examination of PST test observations focused on the detection of cross-polarized fringes to obtain a first-order estimate of the approximate polarization leakage terms (D-terms). No correction for source polarization was applied in these tests. Cross-polarized fringes were first detected in project VT812. Corresponding sample fringe-rate spectra for projects VT824 and VT825 are shown in Figures 1 and 2. These show the cross-polarized fringe-rate spectrum for the phased VLA (Y27) to HALCA baseline for a twenty minute segment of data. The ratio of cross-polarized to parallel-hand coherent amplitudes in each scan is approximately $10-15\%$ at 5 GHz and, $\sim 4\%$ at 1.6 GHz. This provides only an approximate estimate of the order of magnitude of the D-terms, but is instructive nonetheless.

We now discuss the data reduction sequence used for the polarization test observations VT824 and VT825. This is sub-divided into modular sections and aims only to summarize the reduction strategy. Detailed data reduction guidelines will be the subject of a separate document. The data were reduced within the Astronomical Image Processing System (AIPS), maintained by the NRAO.

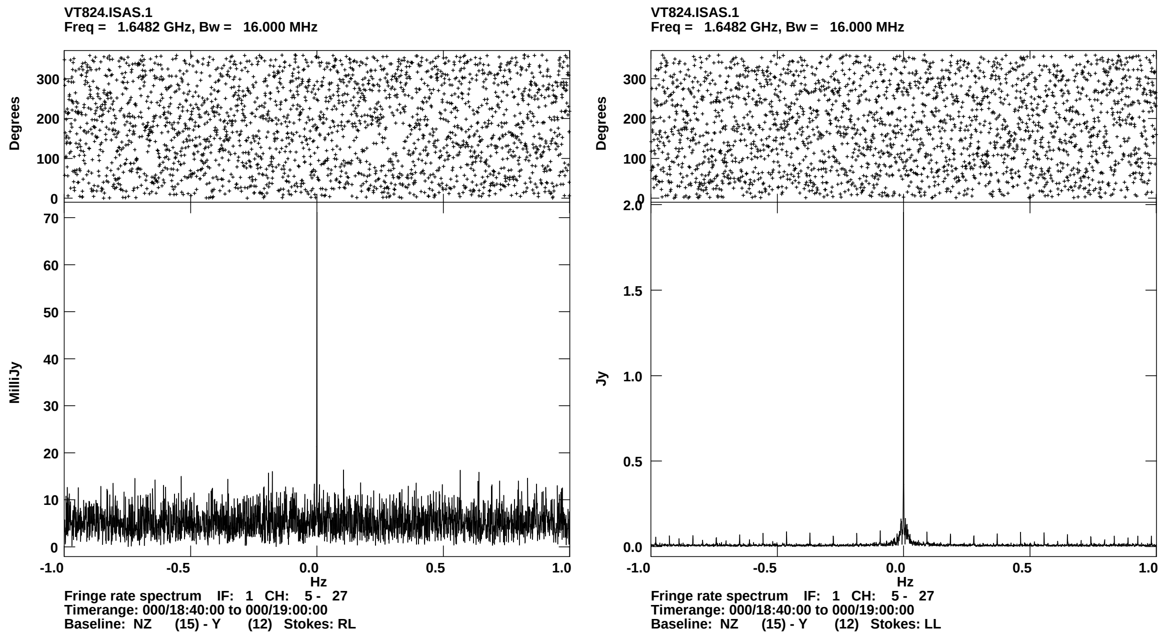

Figure 1: Cross-polarized (RL) and parallel-hand (LL) fringe-rate spectra for the HALCA-Y27 baseline in project VT824, for the time interval 18h40-19h00 and for the single 16 MHz baseband. The data have been calibrated and averaged in frequency over the inner 70% of the band before forming the fringe-rate spectrum from the measured time series of 0.5 s samples. The phase of the fringe-rate spectrum should be ignored in these plots.

4.1 Data loading, examination and initial calibration

The data were loaded on disk using FITLD, applying all digital corrections and scaling appropriate for the VLBA correlator, and rejecting individual uv-data points with a weight below 0.7. Projects VT824 and VT825 were correlated with 128 frequency channels and an integration time of 0.5 s on the space baselines and 2.0 s on the ground baselines. The compressed, concatenated data files had sizes of the order of 3.5-4.5 Gb, which requires large file support ($>$ 2.1 Gb) on the underlying operating system. This is supported by Silicon Graphics, Dec Alpha and Solaris 2.6 operating systems. In practice, the residual delays in these projects permitted a channel spacing four times larger. This point needs to be carefully considered in the correlation of projects of this type, as permitted by the residual delays on the space baselines.

As for all space VLBI data the unequal time sampling leads to a uv-data file out of time-baseline sort order, and with missing calibration and index tables. Task MSORT was used to sort the data into time-baseline order. The calibration and index tables were re-generated using INDXR, with a calibration time sampling of 5 s.

The VLBA output file is TSM format was used to generate the input files for amplitude calibration (ANTAB) and flagging (UVFLG), using task VLOG, after prepending the standard VLBA gain curve information. System temperature and gain information were added to the resultant T_{sys} file for the phased VLA and HALCA. The relevant system temperature information for HALCA for projects VT824 and VT825 is shown in Fig. 3 and Fig. 4. The mean system equivalent flux density for the antennas in each project, expressed in Janskys, is listed in Table 3, as obtained from the measured system temperatures

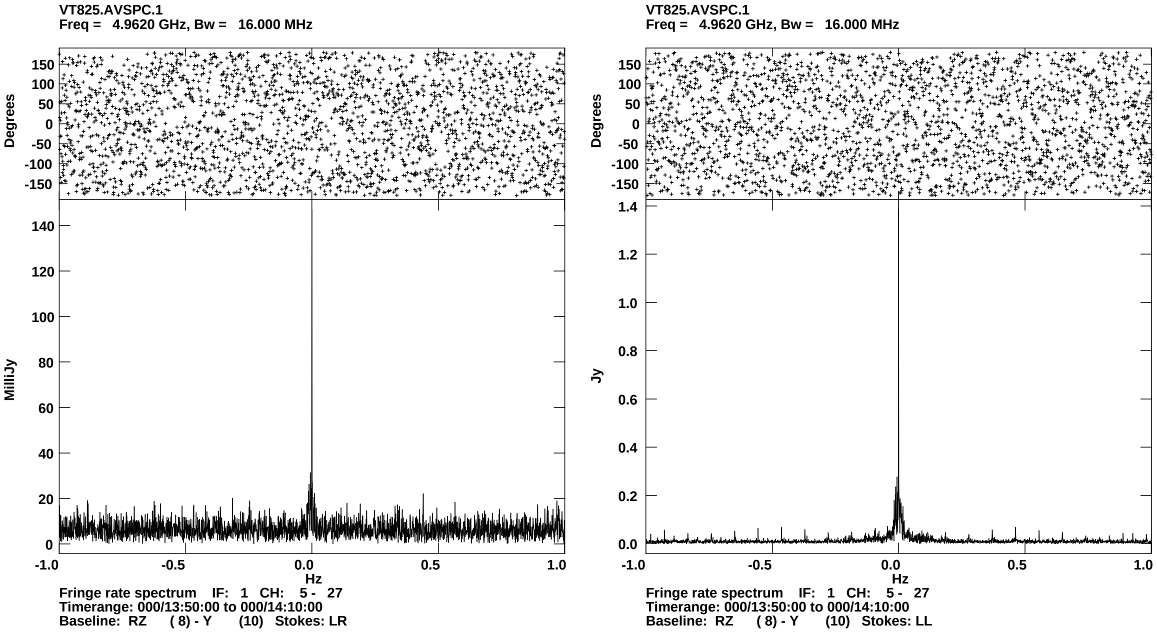

Figure 2: Cross-polarized (RL) and parallel-hand (LL) fringe-rate spectra for the HALCA-Y27 baseline in project VT825, for the time interval 13h50-14h10 and for the first 16 MHz baseband. The data have been calibrated and averaged in frequency over the inner 70% of the band before forming the fringe-rate spectrum from the measured time series of 0.5 s samples. The phase of the fringe-rate spectrum should be ignored in these plots.

and adopted point source sensitivity.

Antenna	SEFD (1.6 GHz) (Jy)	SEFD (5.0 GHz) (Jy)
VLBA	290	310
VLA (Y27)	20	23
HALCA	18300	17600

Table 3: Mean equivalent system temperatures as measured in projects VT824 (1.6 GHz) and VT825 (5 GHz).

The system flags were read in using UVFLG. Additional flags were immediately added to remove the mis-labeled correlations between all ground antennas and HALCA for the missing polarization correlations on the space baselines. The data were examined for completeness using VPLOT, LISTR and DTSUM. An initial parallel-hand fringe-fit was performed using FRING on the 128-channel data, using default global fringe-fitting with baseline-stacking (Schwab and Cotton 1983), taking into account the different time-sampling on the ground and space baselines in order to assess the data quality and determine the delay range at the tracking stations. A solution interval of 1 min was used. Fringes were well detected on the space-baselines in each 16 MHz baseband separately, with a delay range that per-

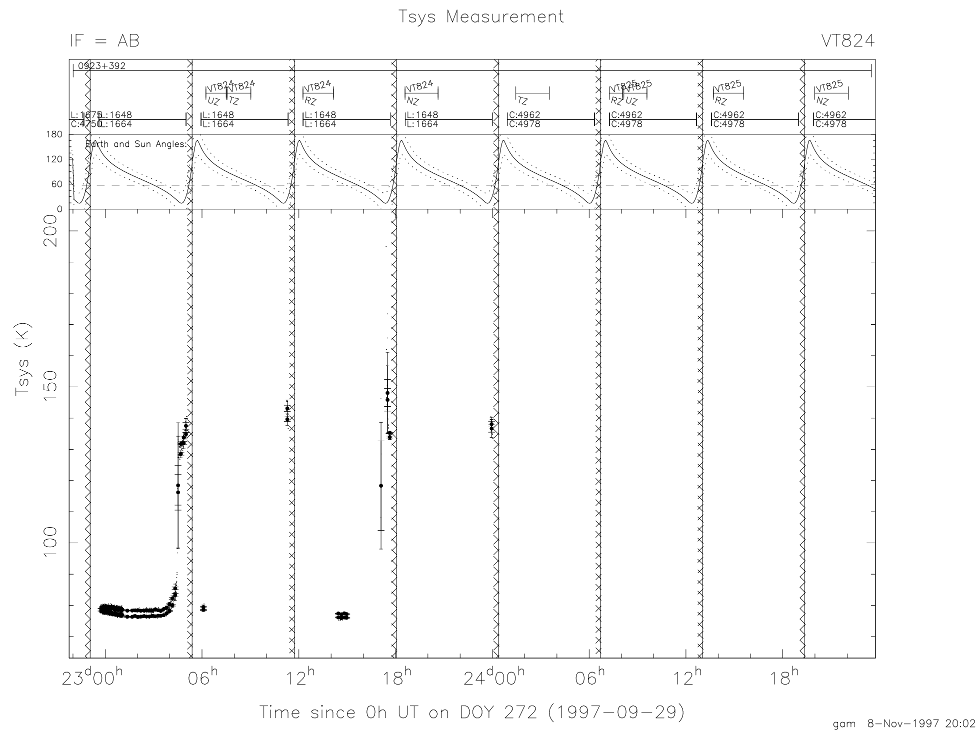

Figure 3: T_{sys} measurements for the HALCA satellite for project VT824

mitted further frequency averaging. This was performed using AVSPC to produce an output file with 32 frequency channels, and which was consequently reduced in size by a factor of four. This file was used in all subsequent reduction.

The a priori amplitude correction factors were determined from the measured system temperatures and adopted point source sensitivities using task APCAL. No ground array opacity corrections were determined or applied. Sampler offset corrections were determined from the mean level of the autocorrelation spectra using ACCOR. These amplitude corrections are of order $5 - 10\%$ and result from offsets in the threshold voltages of the samplers, and need to be corrected for two-bit sampling. The sampler corrections were smoothed over one hour.

Prior to further phase calibration the parallactic angle term was removed from all polarization correlation pairs using task CLCOR. A parallactic angle of zero was assumed for the HALCA antenna. The true parallactic angle for the satellite is absorbed into the measured D-term in this case, as will be discussed further below.

4.2 Initial phase calibration

The phased VLA was adopted as the reference antenna in both projects in all phase calibration.

Prior to any phase calibration, an interim fringe-fit was performed with the same input parameters as given above. These solutions were applied to allow time-averaging during interactive editing with IBLED, and in the bandpass determination discussed below. The resultant flag table was applied in all subsequent reduction.

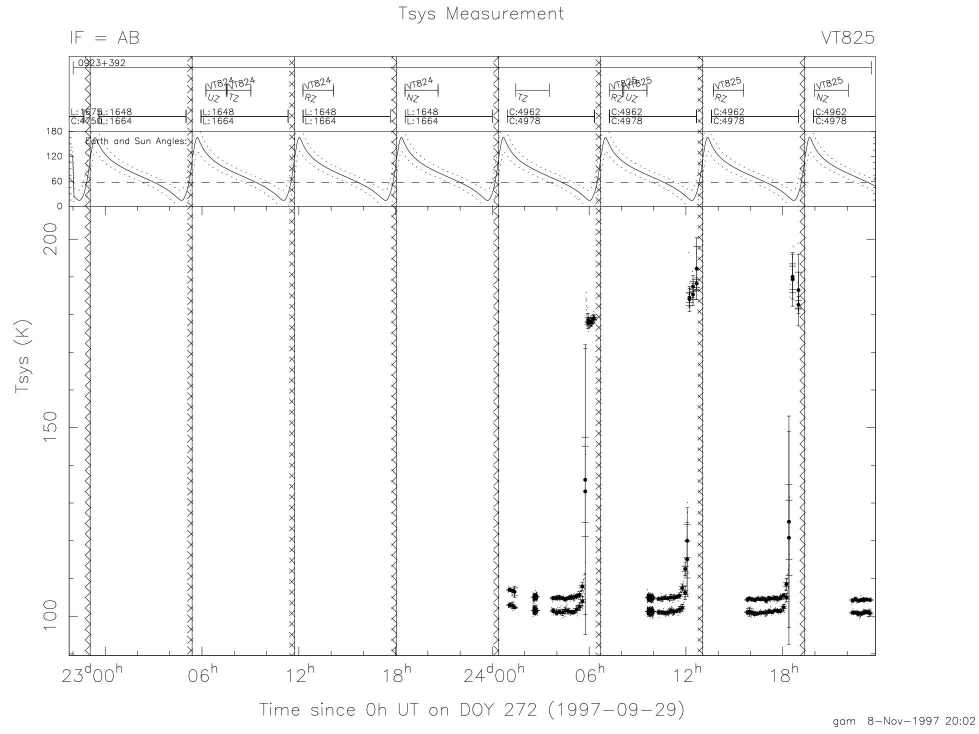

Figure 4: T_{sys} measurements for the HALCA satellite for project VT825

A single bandpass correction was determined for each antenna using task CPASS, which models the complex cross-power bandpass response as a sum of Chebyshev polynomials. The bandpass response is determined using the parallel-hand data alone (RR and LL) and was particularly necessary to correct the first 16 MHz baseband recorded at the phased VLA. The lower edge frequency of the baseband fell too close to the DC edge of the 50 MHz VLA IF, resulting in significant phase excursions (~ 100 degrees) over the first 4 MHz of the band. This was well corrected by the bandpass calibration and is not believed to have introduced any significant effects in further reduction.

A final parallel-hand fringe fit was performed with the updated flag information and after applying the bandpass correction. The solutions were averaged in delay over three minutes, except in HALCA scans in which there were clock jumps leading to delay discontinuities. The solution data were further clipped in rate and delay to remove outliers. The parallel-hand fringe solutions were applied, leaving only the residual R-L phase offset at the reference antenna between the basebands, and the residual R-L delay offset at the reference antenna in each baseband. These were determined by fringe-fitting the cross-polarized data on the PT-Y27 baseline on the target source 4C39.25 using the standard technique. This involves copying out a selected baseline (UVCOP) and applying the parallel-hand phase calibration (SPLIT). Tasks SWPOL, FRING and POLSN were used to derive the R-L delay and phase offsets at the reference antenna, which was chosen to be Y27 in both projects. Thus, delay and phase calibration of orbiting polarization VLBI data is not significantly different from conventional ground-array polarization calibration, as all delay and phase corrections are referred to the ground-based reference antenna.

In project VT825, a R-L delay drift of ~ 7 ns was detected for the phased VLA in the first 16 MHz baseband over the course of the observing run, and was associated with a ~ 30 degree phase drift. This needs to be investigated further as it is not anticipated. It was corrected as measured however and is not believed to have caused any problems in subsequent data reduction. The data need to be reduced with an alternative reference antenna (such at PT) as part of further investigation of this matter. No phase or delay drift was measured at the VLA for project VT824, or in the second baseband of project VT825.

The R-L delay and phase offset calibration completed the initial phase calibration with the exception that the absolute R-L phase difference at the reference antenna was not determined. This is equivalent to stating that the absolute electric vector position angle in the image plane was uncertain by a constant offset. This was corrected at the end of the data reduction and is discussed below. At this point the final amplitude and phase self-calibration could be performed, as all polarization offsets had been removed.

The VLBA and VLA antennas are known to have frequency-dependent polarization leakage. The signature of this effect is sinusoidal amplitude variations in the calibrated cross-polarized cross-power spectra. This is known to affect observations at frequencies below 5 GHz, and is more pronounced at lower frequencies. It was found to be present in both VT824 and VT825. A sample cross-polarized spectrum with this effect is shown in Fig. 5. The signal-to-noise ratio (SNR) of these data, combined with the frequency configuration of the observing mode makes this effect particularly noticeable. It is most likely to be visible in two adjacent 16 MHz baseband channels observed with two-bit sampling. No correction has been made for this effect in the first pass data reduction reported here. The data have been averaged in frequency before final self-calibration, under the expectation that this effect will add errors incoherently into the polarization images when averaged over the array as a whole. This point needs to be explored in further work, using feed calibration software with a frequency dependent model, or by sub-dividing the data in frequency for separate calibration. This effect was also evident in the R-L delay offset estimation for VT824 at 1.6 GHz. The residual reference antenna delays in RL and LR, which should have equal value but opposite sign, did not agree by $\sim 10 - 20$ ns, and a mean value was adopted. Again, this needs to be the subject of further work along the lines discussed above, in modeling the frequency dependence of the polarization leakage terms.

4.3 Self-calibration and imaging

The data were calibrated by applying the amplitude, bandpass, delay, rate and R-L delay-offset corrections, and averaged over the full frequency range using task SPLIT. The inner $\sim 70\%$ of each baseband was used. Task FIXWT was used to provide inverse variance weighting of the resultant output files. The uv coverage for projects VT824 and VT825 is shown in Fig. 6.

Self-calibration and imaging of the Stokes I data was performed using SCMAP and standard hybrid-mapping techniques. Initial phase self-calibration was followed later by amplitude self-calibration to produce the final maps. Interactive editing was performed as required throughout the self-calibration iterations. The self-calibration and imaging parameters are listed in Table 4.

The final Stokes I images for VT824 and VT825 are shown in Fig. 7 and Fig. 8. Please note that the scientific rights to the 5 GHz total intensity image are the property of Alberdi *et al.* and Lobanov *et al.* , the AO 1 proposers of this source at this frequency. In forming Stokes Q and U images, complex imaging and deconvolution is required, as discussed above, due to the unequal sampling in RL and LR on the space baselines. This was performed using tasks UVPOL and CXCLN. In what follows the linearly polarized intensity is denoted by $P = \sqrt{(Q^2 + U^2)}$.

4.4 Feed calibration

As an initial approach to feed calibration, a standard polarization calibration technique used for ground array observations was applied, as implemented in task LPCAL (Leppanen 1995). In this approach the unknown polarization structure of the source is modeled by separating the Stokes I image into a small

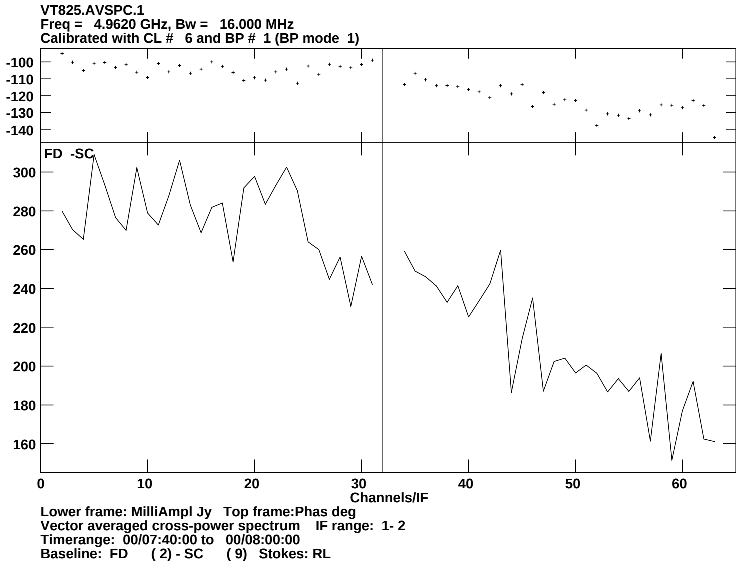

Figure 5: Cross-polarized cross-power spectrum on the baseline FD-SC for project VT825 after initial phase calibration, for the time interval 07h40-08h00.

number of discrete components. The polarized emission is assumed to be a constant complex fraction of the Stokes I emission (Cotton 1993) for each component and the unknown scaling coefficients are estimated in a joint solution for antenna-based D-terms.

In the case of VT824 and VT825, the Stokes I CLEAN component model was automatically decomposed into two components using task CCEDT. We consider the results of feed calibration for the two projects separately:

4.4.1 VT824

The target source 4C39.25 has very low polarization at 1.6 GHz on VLBI scales. A polarization image obtained using only the ground array data from VT824 revealed essentially no detected linear polarization. This was true also of the map using all data including the space baselines. The ground-array D-terms were found to be $\leq 4\%$ in amplitude at this frequency, as expected, with a mean value of $\sim 1.0 - 1.5\%$. The uncalibrated P image for project VT824, using all data including the space baselines, is shown in Fig. 9.

This project has three separate tracking passes, and as a first approach the HALCA D-term was determined separately for each tracking pass. This produced estimates of the D-term amplitude in the range [2.4,4.9]% but these estimates were clearly limited by SNR on the space baselines. The integrated flux density of 4C39.25, as determined by the simultaneous phased VLA data, is 3.6 Jy, and the correlated LL amplitude on the space baselines was typically less than 1 Jy. In a second feed calibration test, the tracking pass data were combined as one antenna using task RESEQ, and a single composite D-term estimated. A D-term amplitude of $\sim 2.3\%$ was obtained with a phase of ~ 120 degrees. The D-term estimate for VT824 is limited by the SNR of the data in this project and may be uncertain by up to a factor of two. There is insufficient SNR to estimate the time variability of the D-term and we can make

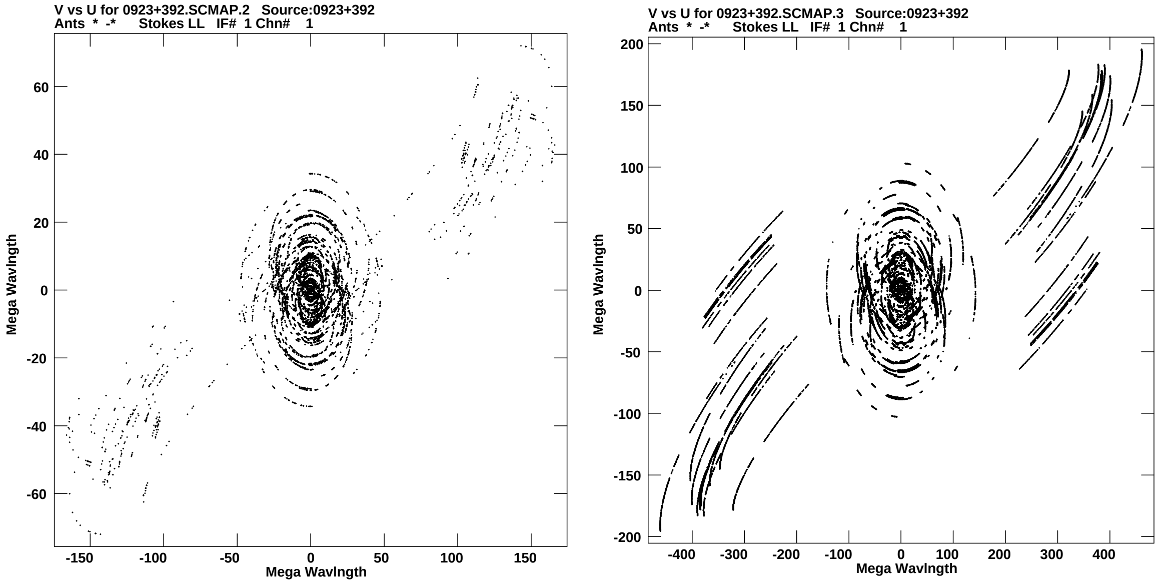

Figure 6: The uv-coverage for projects VT824 (left panel) and VT825 (right panel).

no statement here in that regard. Further observations of compact sources with higher correlated flux density on the space baselines would permit a more accurate estimate of the polarization leakage at 1.6 GHz and its time variability.

Note that the D-term phase needs to be corrected for the actual HALCA parallactic angle if comparing it to D-terms estimated from other observations. The simultaneous estimate of the HALCA D-term was not found to significantly bias the estimated ground array D-terms. The calibrated polarization image including the HALCA D-term correction is shown in Fig. 10.

Separate confirmation of the D-term amplitude was obtained by applying polarization calibration for the ground array and then taking the ratio of the cross-polarized to parallel-hand data on the HALCA baselines and averaging over intervals up to 30 min. A comparable amplitude ratio is obtained. We note also that the D-term amplitude is consistent with the cross-polarized fringe-rate spectra plotted for VT824 above.

The effect of feed calibration on the Y27-HALCA baseline at 1.6 GHz is illustrated in Fig. 11, where the real and imaginary parts of the cross-polarized data on this baseline are plotted on an Argand diagram, with and without polarization calibration. Polarization calibration of both Y27 and HALCA removes the offset due to the instrumental polarization, and is consistent with the low polarization measured in the VLBI data.

4.4.2 VT825

The polarization image for the target source 4C39.25 at 5 GHz, as obtained from the ground array VT825 data alone, is shown in Fig. 12. The degree of linear polarization is of the order of $\sim 1\%$. The simultaneous VLA data yield an integrated flux density estimate for the source of 11.4 Jy. The ground array image shows evidence of significant polarization structure near the core but this structure is not clearly resolved. The ground array D-terms are $\leq 2\%$ with a mean amplitude of $\sim 1\%$ as expected.

Parameter	VT824 (1.6 GHz)	VT825 (5 GHz)
Cell size	0.2 mas	0.1 mas
Image weighting	Uniform	Uniform
Noise limit	1.7 mJy/beam	1.2 mJy/beam
Actual noise	2.3 mJy/beam	6.6 mJy/beam
Beam	5.36 x 1.12 mas PA -14.9 deg	1.53 x 0.3 mas PA -13.0 deg

Table 4: Self-calibration and imaging parameters for VT824 and VT825.

The uncalibrated polarization image for VT825, using all data including the space baselines, is shown in Fig. 13.

Using the same feed calibration technique as used in VT824 leads to an estimate for the HALCA D-term of 11% in amplitude with a phase of ~ -46 degrees. As before, CCEDT was used to automatically decompose the Stokes I image into two components, which were then used in LPCAL. Simultaneous estimation of the HALCA D-term was not found to significantly bias the estimated ground array D-terms, as obtained from the ground array data alone. As in project VT824, the phase of the HALCA D-term needs to be corrected for the parallactic angle of the spacecraft for this observation if it is to be compared to values obtained from other projects. The calibrated polarization image including HALCA is shown in Fig. 14. The effect of calibrating only the ground array is shown in Fig. 15. A comparison of Fig. 14 and Fig. 15 shows that the HALCA D-term correction leads to a significant improvement in the quality of the polarization image. The absolute electric vector position angle was determined using the simultaneous VLA data, referred to the known polarization position angle for 3C286, and transferred to the VLBI data via the compact source DA193. We note that this map is consistent with the ground array 15 GHz polarization map reported by Alberdi *et al.* 1998, and that the HALCA baselines clearly separate the two polarized components near the core.

In the joint solution for the HALCA and ground array D-terms, the effect of varying the uv-range of the selected input data was explored. The rationale behind this approach is to exclude the longer space baselines in the feed solution so that the polarization model is less vulnerable to uncertainties in the fine scale structure, for which there is only information on the space baselines. Data within a uv-range of 0-200$k\lambda$ and 0-250$k\lambda$ were used as well as data with no uv-range limit, with a worst-case variation in the estimate of the D-term amplitude of $\sim 2\%$ (from 9-11%) and D-term phase of ~ 25 degrees. The typical variation was $\pm 1\%$ in amplitude and ~ 15 degrees in phase, which is not significant in this context. Note that the fraction of data to HALCA used in the solution was significantly reduced by the uv-range selection.

There was insufficient data to accurately estimate time variability of the D-term solution. Solving for a HALCA D-term for each tracking pass separately did not show any evidence of significant variability. The two tracking passes were separated by $\sim$5h40m, and occur at roughly the same orbital phase.

The effect of calibrating the Y27-HALCA baseline for instrumental polarization is shown in Fig. 16, where the real and imaginary parts of the cross-polarized data on this baseline are plotted in a Argand diagram, with and without polarization calibration. The effect of polarization calibration is to remove the offset in the weighted mean position of the data in this plane.

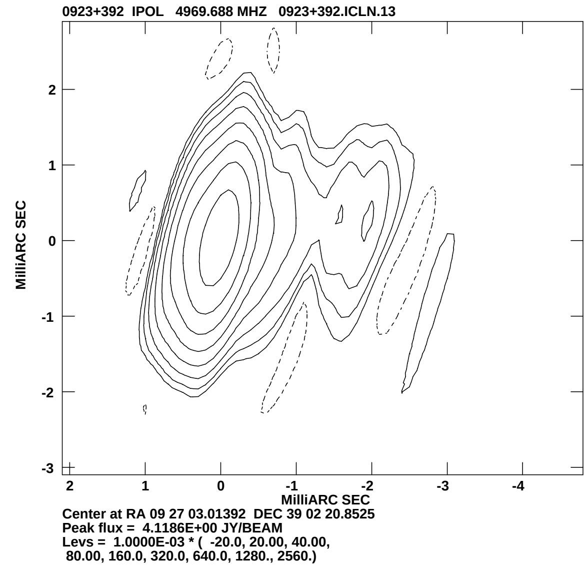

Figure 7: Stokes I image for project VT825, using all baselines. For imaging parameters see section 4.3. Please Note: The scientific rights to this 5 GHz total intensity image are the property of Alberdi *et al.* and Lobanov *et al.* , the AO 1 proposers of this source at this frequency.

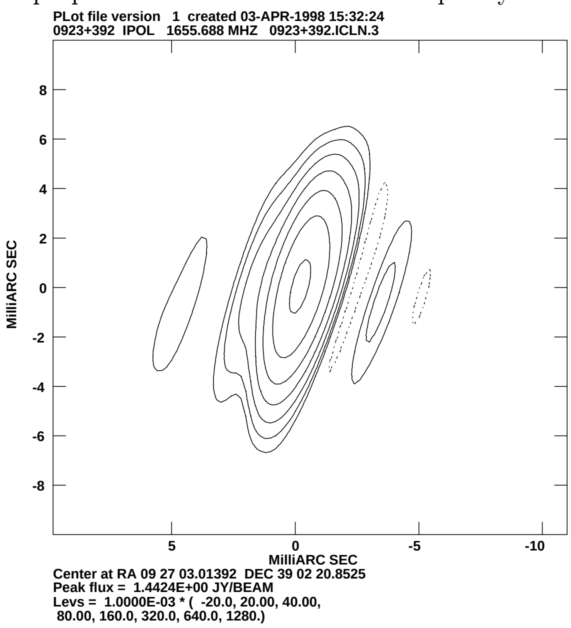

Figure 8: Stokes I image for project VT824, using all baselines. For imaging parameters see section 4.3.

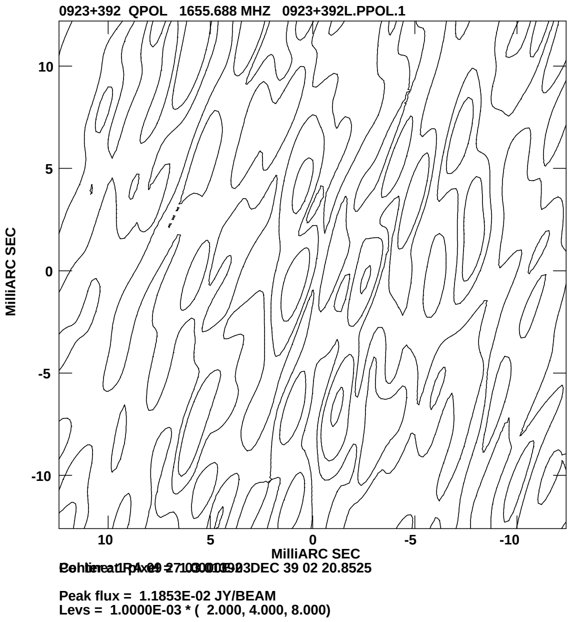

Figure 9: P image for project VT824, using all baselines. No feed calibration has been applied in this case.

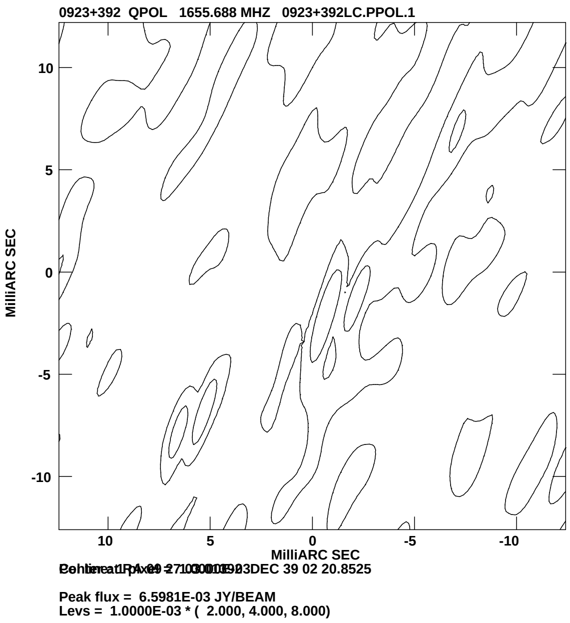

Figure 10: Calibrated P image for project VT824, including all baselines, and using one D-term to correct the HALCA data. This figure is plotted with the same contour levels as Fig. 9.

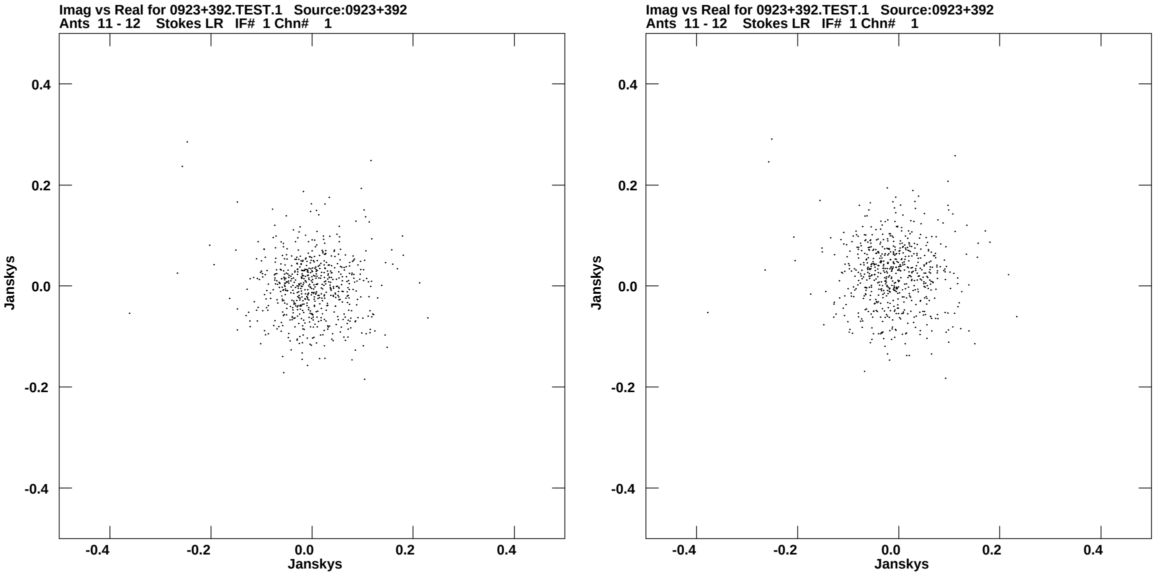

Figure 11: Plots of the real versus imaginary components of the cross-polarized data on the Y27-HALCA baseline for project VT824, with (left panel) and without feed calibration (right panel).

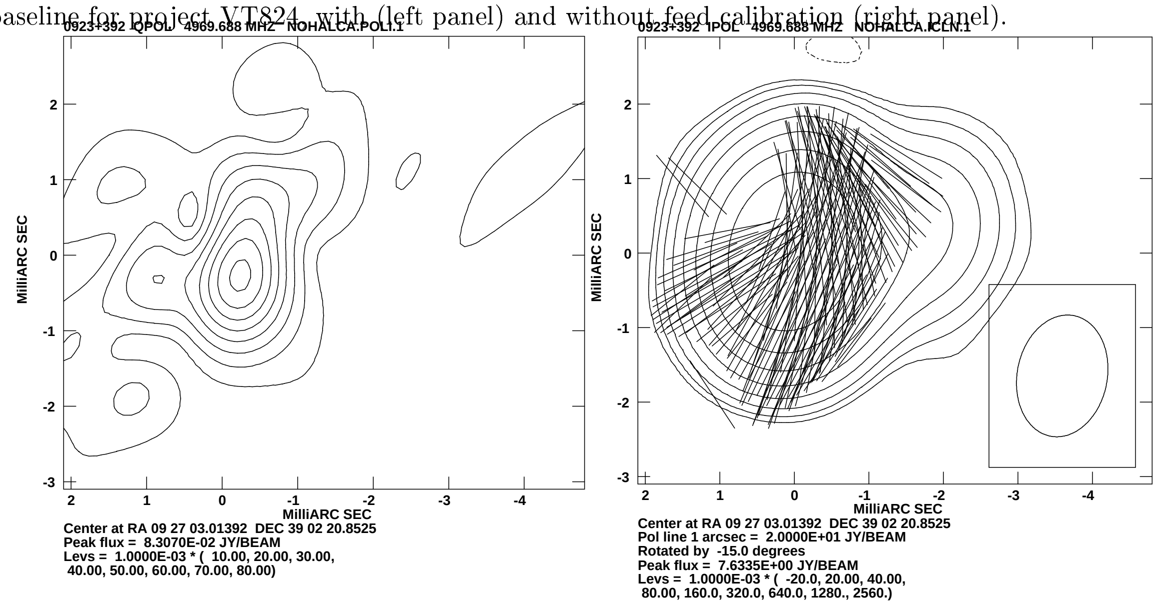

Figure 12: Calibrated P image for project VT825, using all baselines (left panel). A contour plot of Stokes I is shown on the right, superimposed with electric vectors of length proportional to P. Please Note: The scientific rights to the 5 GHz total intensity image are the property of Alberdi *et al.* and Lobanov *et al.* , the AO 1 proposers of this source at this frequency.

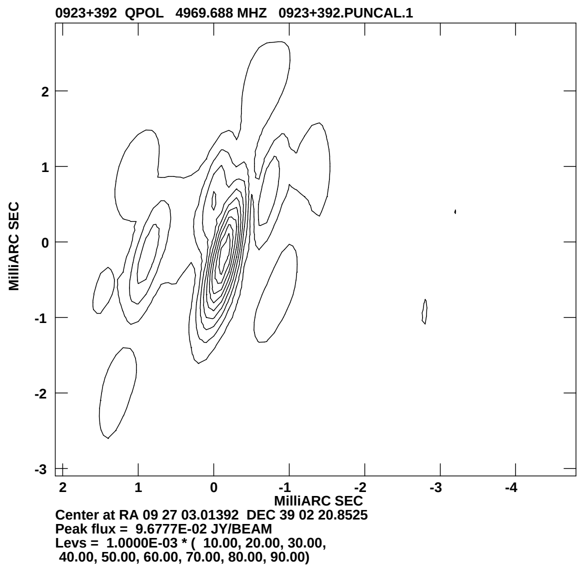

Figure 13: P image obtained for project VT825, using all data including space baselines. No feed calibration has been applied in this case.

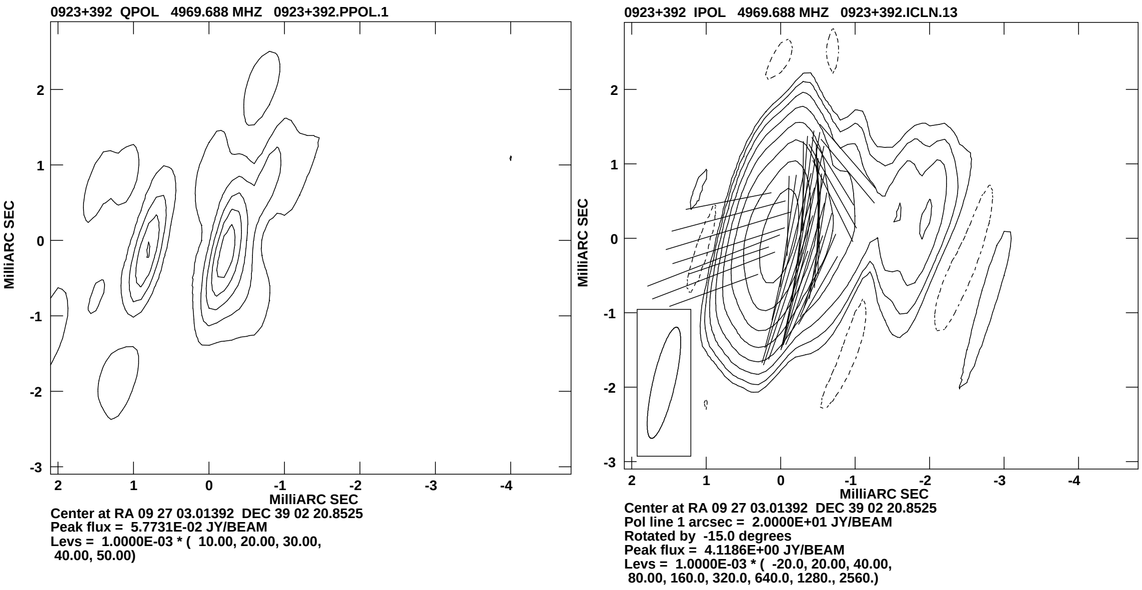

Figure 14: Calibrated P image for project VT825, using all data including space baselines (left panel). A contour plot of Stokes I emission is shown in the right panel, superimposed with electric vectors of length proportional to the linearly polarized intensity. Please Note: The scientific rights to this 5 GHz total intensity image are the property of Alberdi *et al.* and Lobanov *et al.* , the AO 1 proposers of this source at this frequency.

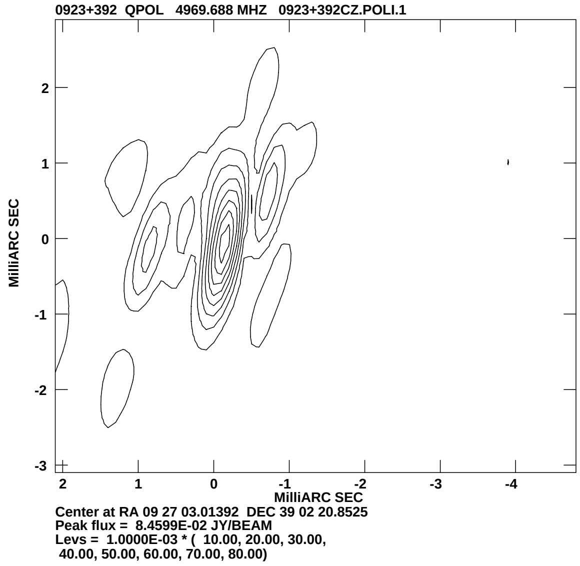

Figure 15: P map for project VT825, using all data including the space baselines, but with feed calibration applied only for the ground antennas. The same contours levels are used as in Fig. 14 and Fig. 9.

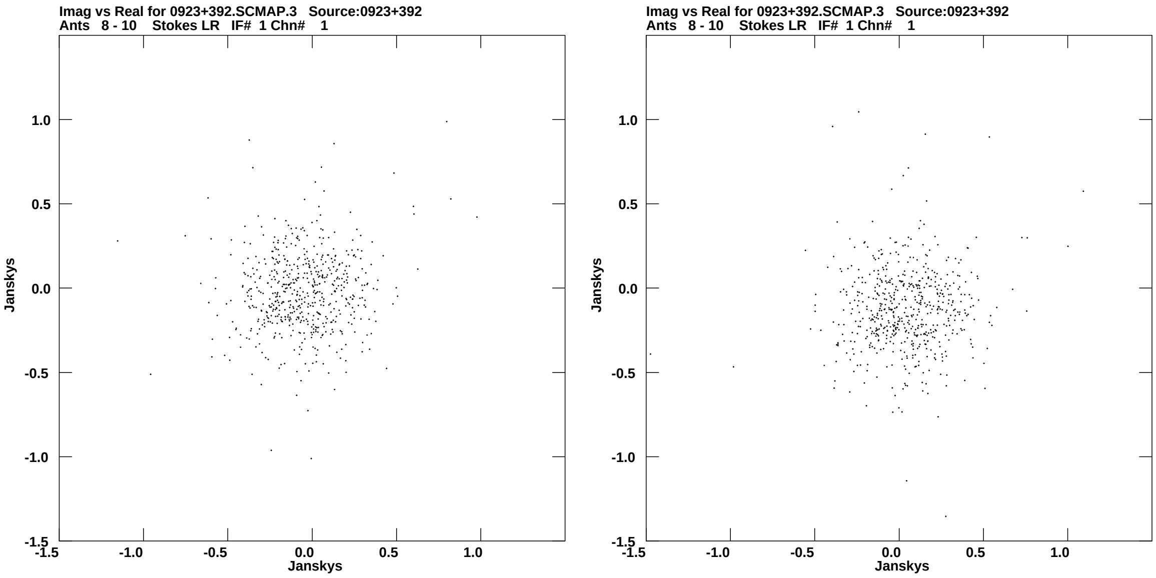

Figure 16: Plots of the real versus imaginary components of the cross-polarized data on the Y27-HALCA baseline for project VT825, with (left panel) and without (right panel) feed calibration.

5 Discussion and conclusions

The following discussion is based primarily on experience in reducing test observations VT824 and VT825. In this regard we raise the following points:

- **Feasibility of HALCA polarization observations:** The magnitude and variability of the D-terms, as estimated at 1.6 GHz and 5 GHz from projects VT824 and VT825, appears to be sufficiently low to allow polarization observations with HALCA of sources with sufficient correlated polarized flux density. The effective correlated polarized flux density limit for feasible HALCA polarization observations is not known precisely, however a conservative limit would probably be 5-7σ. The polarization map of 4C39.25 at 5 GHz obtained here is consistent with the existing 15 GHz ground array image at comparable spatial resolution. The scientific benefit of high-resolution centimeter polarization imaging with HALCA is technically within reach.
- **Feed calibration strategies:** For 4C39.25, the default polarization calibration strategy was sufficient to estimate the D-term. More sophisticated approaches did not significantly improve the quality of the polarization calibration in this case. This will remain to be seen in the reduction of PST test observations with sources that have more extended structure or lower SNR than 4C39.25.
- **Time variability of HALCA's instrumental polarization:** There is no conclusive evidence on this point given the limited tracking in parts of VT824 and VT825. However, the 5 GHz observations show little evidence for significant variability over more than 5 hours. Variability as a function of orbital phase could not be explored. Further reduction of PST test observations will provide more insight into this question.
- **Frequency dependence:** The influence of the frequency dependence of the polarization response of the ground antennas needs to be investigated using a more sophisticated D-term model, and in follow-up ground observations in a narrower bandwidth.
- **Future work:** The reduction of PST test observations will continue, using data taken in December 1997 and later. These projects have been scheduled as part of the General Observing Time (GOT) but will provide important insight into some of the remaining questions raised above.

6 References

Alberdi *et al.* , 1993, ApJ, 402, 160.
Alberdi *et al.* , 1998, in IAU Colloq. 164, in press.
Cotton, W.D. *et al.* , 1984, ApJ, 286, 503.
Cotton, W.D., 1993, AJ, 106, 1241.
Gabuzda, D. *et al.* , 1992, ApJ, 388, 40.
Kemball, A. *et al.* , 1995, AA Suppl., 110, 383.
Kogan, L., 1997, AIPS Memo. 93.
Leppanen, K., Ph.D. thesis, Helsinki University of Technology.
Marcaide, J.M. *et al.* , 1994, in Compact Extragalactic Radio Sources (eds. Zensus and Kellermann), p141.
Roberts, D. *et al.* , 1984, in IAU Symp. 110 (eds. Fanti, Kellermann and Setti),
Roberts, D. *et al.* , 1994, ApJ, 427, 718.
Schwab, F.R. and Cotton, W.D., 1983, AJ, 88, 688.